

Microstructure and mechanical properties of an Al–Ni–Co intermetallics reinforced Al matrix composite

Suling Cheng · Gencang Yang · Jincheng Wang ·
Changlin Yang · Man Zhu · Yaohe Zhou

Received: 7 December 2008 / Accepted: 31 March 2009 / Published online: 20 April 2009
© Springer Science+Business Media, LLC 2009

Abstract A new intermetallic particle reinforced metal matrix composite was produced from pure Al and 15 wt% $\text{Al}_{72}\text{Ni}_{12}\text{Co}_{16}$ quasicrystalline particles by stir-casting method, followed by hot-extrusion. Microstructural analysis of the as-cast composite shows that the $\text{Al}_{72}\text{Ni}_{12}\text{Co}_{16}$ quasicrystalline phase has transformed to the crystalline phase $\text{Al}_9(\text{Co}, \text{Ni})_2$ and an eutectic structure has formed in the Al matrix during the casting process. The particle size of the $\text{Al}_9(\text{Co}, \text{Ni})_2$ phase is much smaller than that of the original quasicrystalline particles. After extrusion, the composite has a more uniform distribution of the reinforcement particles and eutectic structure as well as a reduced porosity. Tensile tests indicate that the mechanical properties of the as-cast composite are improved over the matrix properties remarkably, except for the ductility. The strength and ductility of the composite can be improved by the hot-extrusion, while the elastic modulus can be slightly decreased.

Introduction

Aluminum matrix composites (AMCs) reinforced with ceramic particles have been much developed as wear-resistant and structural materials due to their attractions of low density, wide alloy range, heat treatment capability, and processing flexibility [1]. However, several difficulties, such as poor wettability, difficulty of recycling, and

interfacial reactions, have been encountered during the fabrication and application process of the composites. Those difficulties motivate the development of alternative reinforcement materials.

Quasicrystals (QCs) as a kind of intermetallic compounds (IMCs), provide a superior wettability and a closer coefficient of thermal expansion with Al as compared with ceramic materials while possess comparable mechanical properties [2]. Consequently, some efforts were recently initiated by several research groups to use QC (Al–Cu–Fe) as the particle reinforcement for AMCs fabricated by conventional casting process, powder metallurgy, and mechanical alloying techniques [3–6]. It was found that in Al melts or when consolidation temperature was higher than 500 °C, diffusion reactions between the Al matrix and the Al–Cu–Fe quasicrystalline particles took place, and the quasicrystalline phase transformed to the crystalline phase $\text{Al}_7\text{Cu}_2\text{Fe}$, which has a higher Al content as compared with that in the quasicrystalline phase (63–65at.% Al) [3–6]. These results suggest that, since no quasicrystalline phase coexisting with Al phase in the corresponding equilibrium ternary phase diagram has been found yet, diffusion reactions between quasicrystalline particles and Al matrix are inevitable in a solid/liquid state even in a solid/solid state at high temperatures. However, despite the phase transformation of the quasicrystalline particles, the mechanical properties of the resultant composites were remarkably improved over the matrix properties, and the strengthening efficiency was found to be equivalent to or even exceed that of ceramic particles [3–6]. This unusual strengthening effect was explained to be attributed to several factors including [4–6]: (i) mechanical and physical property similarities between the resultant crystalline particles and the original quasicrystalline particles; (ii) uniform distribution of the reinforcement particles in the matrix due to

S. Cheng (✉) · G. Yang · J. Wang · C. Yang · M. Zhu ·
Y. Zhou

State Key Laboratory of Solidification Processing, Northwestern
Polytechnical University, 710072 Xi'an, China
e-mail: chengsuling@163.com

the good wettability; (iii) integrated particle–matrix interfacial bonding arising from the diffusion reaction as well as the good wettability; and (iv) matrix strengthening due to element diffusion from the particles to the matrix.

However, the Al–Cu–Fe particles used in Ref. [4] are multiphase alloy, and no article concerning adding single-quasicrystalline phase particles to metal matrix by casting method has been found. It is expected that different results would be obtained if single-quasicrystalline particles were to be added to Al matrix by stir-casting method, since the coexisting phases can affect the reaction process between quasicrystalline particles and Al matrix and, thereby, affect the microstructure and finally the mechanical properties of the resultant composite. This article deals with this research work.

According to Tsai et al. [7], $\text{Al}_{72}\text{Ni}_{12}\text{Co}_{16}$ is one of the most stable QCs and the single-quasicrystalline phase alloy can readily be produced. Therefore, $\text{Al}_{72}\text{Ni}_{12}\text{Co}_{16}$ was chosen as the particle reinforcement for pure Al matrix in this study. Since the $\text{Al}_{72}\text{Ni}_{12}\text{Co}_{16}$ quasicrystalline phase also can not coexist with Al phase according to the corresponding ternary diagram [8], diffusion reaction is expected to occur when the quasicrystalline particles are mixed into the Al melt. This article aims to characterize the microstructure and tensile properties of the resultant composite. Moreover, hot-extrusion experiments were carried out on the as-cast composite to evaluate the effect of the secondary process on the composite microstructure and mechanical properties.

Materials and experimental procedure

The alloy with the nominal composition of $\text{Al}_{72}\text{Ni}_{12}\text{Co}_{16}$ was prepared by induction melting the constituent pure metals under an argon atmosphere. The microstructure of the produced alloy was examined by X-ray diffraction (XRD), scanning electron microscopy (SEM), and transmission electron microscopy (TEM). The results confirmed that the alloy consists of only one phase, whose selected area diffraction patterns showed 10-fold symmetry characterizing of decagonal QC (not shown in this article). The QC ingot was then crushed using a ball mill and sieved. Particles within the size range of 100–150 μm were used for synthesizing composite. The appearance of the as-prepared quasicrystalline particles is shown in Fig. 1a. It can be seen that many dust is adsorbed on the particle surface, which is deleterious to the wetting process, when the particles are mixed into the molten Al. The dusts were mostly eliminated after the particles were washed in acetone as shown in Fig. 1b. The facet morphology of the particles in Fig. 1a, b indicates the brittle fracture character, confirming the inherent brittleness of the quasicrystalline alloy.

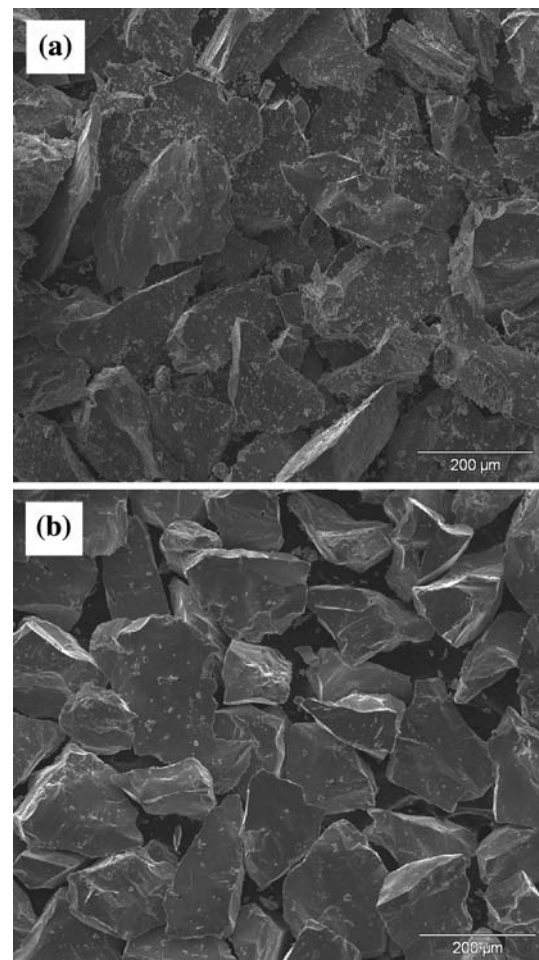


Fig. 1 Morphologies of the Al–Ni–Co quasicrystalline particles in the size range of 100–150 μm in as-prepared state (a) and after wash in acetone (b)

For synthesizing composite, commercial pure Al (99.8%) was melted in a graphite crucible using an electrical resistance furnace and refined at a proper temperature. The quasicrystalline particles were preheated at 500 $^{\circ}\text{C}$ to avoid the chilling effect on the Al melt during the particle loading process. The quasicrystalline particles (15 wt%) were added to the Al melt at 670 $^{\circ}\text{C}$ (slightly higher than the melting point of pure Al) using mechanical stirring method in about 3 min. After the particle loading, the temperature of the slurry was slightly decreased to around 650 $^{\circ}\text{C}$ due to the low temperature of the particles. Here, the Al matrix keeps its liquid state at 650 $^{\circ}\text{C}$ due to the dissolution of elements Ni and Co from the Al–Ni–Co particles. Stirring was continued at this temperature for another 2 min. Then, the slurry was rapidly heated up to 700 $^{\circ}\text{C}$, stirred for 5 min to avoid the settling of the particles, and followed by pouring into a preheated (340 \pm 10 $^{\circ}\text{C}$) steel mold. In order to produce as-cast samples and samples for extrusion, the steel molds with

length of 120 mm, diameter of 18 mm and 36 mm, respectively, were used. As-cast pure Al was also prepared in a similar way for comparison. The prepared composite samples were homogenized at 400 °C for about 2 h, and subsequently extruded at 400 °C with a reduction ratio of 9:1.

The microstructures were analyzed by SEM, XRD, and TEM. In order to roughly evaluate the porosity level of the composite in as-cast state and after extrusion, the density of the composite was measured by a water displacement method and compared with the value calculated based on the rule of mixtures (ROM) [9].

Tensile tests were performed at a strain rate of 0.3 mm/min on round specimens with a diameter of 5 mm and gauge length of 25 mm at the room temperature. Fractographs and longitudinal-section microstructures near the fracture surface of the tensile samples were examined by SEM.

Results and discussion

Microstructure of the as-cast composite

A typical microstructure of the as-cast composite is shown in Fig. 2a. Polygonal morphology particles (PP), Al matrix (AM), and eutectic phases (EP) formed in the interdendritic region are clearly shown in the figure. The polygonal particles distribute randomly both in the Al grains and along the grain boundaries. Although pockets of particle-rich and particle-free regions can be observed in the as-cast composite (Fig. 2a), particle-porosity cluster, a prevailing microstructure defect in ceramic particle reinforced AMCs [10–14], especially when they were produced by casting method, can not be found. It is striking to note that the size of the polygonal particles in the Al matrix mostly falls in a range of 15–25 μm , which is much smaller than that of the original quasicrystalline particles (100–150 μm). Although a small amount of much larger particles can also be found, the maximum size does not exceed 50 μm . In order to observe the particle–matrix interfacial morphology, TEM analysis was carried out on the as-cast sample. As shown in Fig. 2b, the particle–matrix interfacial zone appears to be defect free with no air bubbles, voids, or cracks, exhibiting a perfect metallurgical interfacial bonding.

The results described above show that totally 10 min stirring time is sufficient to disperse the Al–Ni–Co particles uniformly into the Al melt. Usually, at least 20 min are necessary to disperse exceeding 10 vol.% ceramic particles into an Al melt and some alloying elements such as Mg, Cu has been used to promote wetting [1, 15–20]. This is due to the superior wettability between the IMC particles and the molten Al. On the other hand, the particles acting as

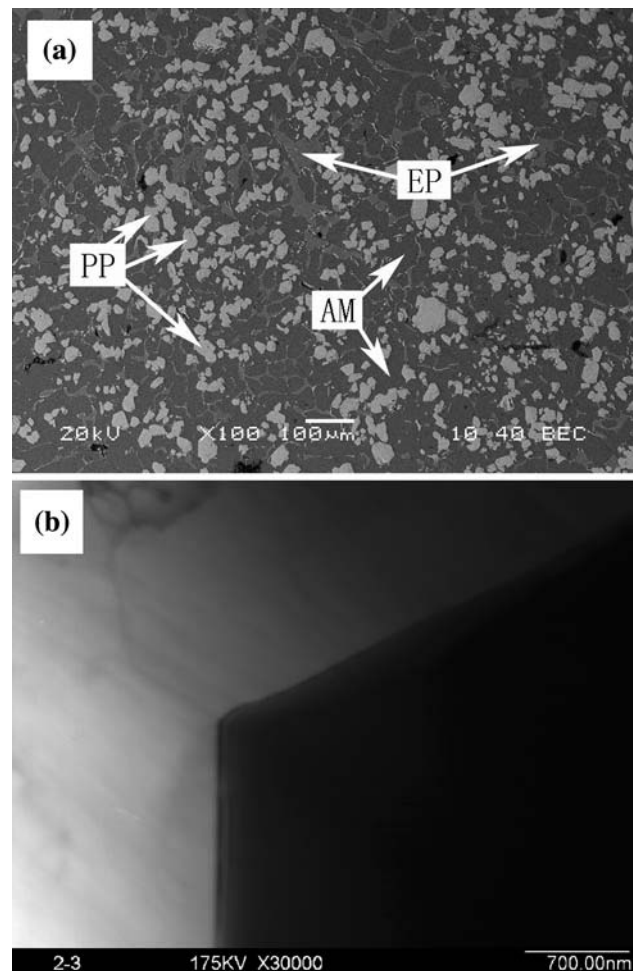


Fig. 2 Backscattered electron (BSE) image of the as-cast composite (a) and transmission electron microscopy (TEM) image showing a typical particle–matrix interface in the as-cast composite (b)

heterogeneous nucleation sites for primary Al phase are captured by growing Al crystals, and finally stay within the Al grains in the composites. This phenomenon can be responsible for the presence of a large number of particles within the matrix grains (see Fig. 2a). The composition of the polygonal particle and its origin as well as its smaller particle size will be discussed hereinafter.

Figure 3a, b is the XRD patterns of the original quasicrystalline particles and the as-cast composite, respectively. It is confirmed by Fig. 3a that the original quasicrystalline particles have a single-quasicrystalline structure. As for the as-cast composite, besides the Al phase, two crystalline phase, $\text{Al}_9(\text{Co}, \text{Ni})_2$ and $\text{Al}_3(\text{Ni}, \text{Co})$, were detected, but no $\text{Al}_{72}\text{Ni}_{12}\text{Co}_{16}$ quasicrystalline phase can be found (Fig. 3b). Energy dispersive spectroscopy analysis showed that the composition of the Al–Ni–Co particles altered from original 72–12–16 to 82–4–14 (at.%), which confirmed that the polygonal phase in the Al matrix should be the $\text{Al}_9(\text{Co}, \text{Ni})_2$ crystal. According to the

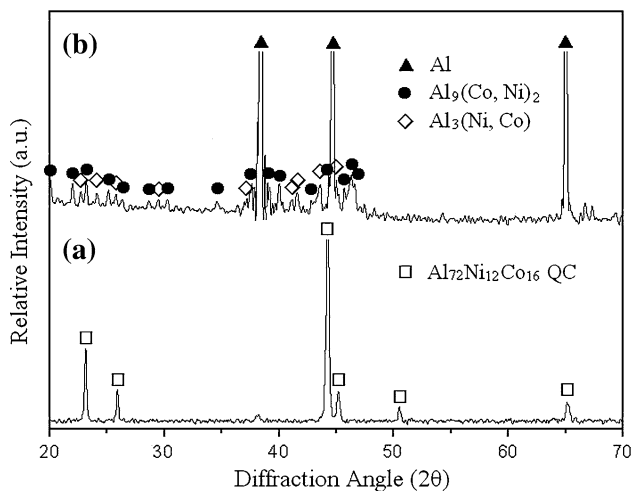


Fig. 3 XRD patterns of the original $\text{Al}_{72}\text{Ni}_{12}\text{Co}_{16}$ quasicrystalline particles (a) and the as-cast composite (b)

Al–Ni–Co ternary phase diagram [8] together with the XRD analysis results, the eutectic phases formed in the interdendritic region (Fig. 2a) should be Al, $\text{Al}_3(\text{Ni}, \text{Co})$, and $\text{Al}_9(\text{Co}, \text{Ni})_2$ ternary eutectic.

A comparison has been made between the microstructures of the as-cast composite obtained in the present study and that in Ref. [4]. Despite the materials and experimental procedure used here are similar to those in Ref. [4], the resulting microstructures are rather different. In Ref. [4], the size of the Al–Cu–Fe particles kept constant and the quasicrystalline phase in the particles was remained, in spite of slightly dissolution of the small Al–Cu–Fe particles and decrease of the quasicrystalline phase volume fraction in the particles. In the present case, however, the quasicrystalline phase has transformed completely and the particle size is decreased remarkably.

According to the Al–Ni–Co ternary phase diagram [8], Al/ $\text{Al}_{72}\text{Ni}_{12}\text{Co}_{16}$ is a non-equilibrium system, and the phases, which can present equilibrium with Al phase, are $\text{Al}_9(\text{Co}, \text{Ni})_2$ and $\text{Al}_3(\text{Ni}, \text{Co})$ in thermodynamics. Therefore, the interactions between $\text{Al}_{72}\text{Ni}_{12}\text{Co}_{16}$ quasicrystalline particles and the Al melt are inevitable during the mixing process, which results in a mixture composed of $\text{Al}_9(\text{Co}, \text{Ni})_2$ particles and liquid Al dissolved with Ni and Co. During solidification, the liquid undergoes the eutectic reaction at 637.9 °C [21], forming Al matrix with ternary eutectic phase (Al, $\text{Al}_9(\text{Co}, \text{Ni})_2$ and $\text{Al}_3(\text{Ni}, \text{Co})$) distributing along the grain boundaries. The smaller particle size of the $\text{Al}_9(\text{Co}, \text{Ni})_2$ phase is considered to be due to the fragmentation of the reaction product owing to the combined effects of heat impact, reaction stress, and the stirring action, etc. In Ref. [4], as aforementioned, the Al–Cu–Fe particles used are multiphase alloy. Maybe due to the effect of the coexisting crystalline phases in the Al–Cu–Fe

particles, which can act as diffusion reaction barriers to block the reaction between the quasicrystalline phase and the molten Al, the quasicrystalline phase remained and the particle size kept constant as the casting time was sufficiently short.

The diffusion reaction of the Al/ $\text{Al}_{72}\text{Ni}_{12}\text{Co}_{16}$ system was found to be very fast. The formation of the $\text{Al}_9(\text{Co}, \text{Ni})_2$ reaction product and its fragmentation occurred and completed only in no more than 20 s under stirring at a temperature close to the melt point of the matrix. The interactions between the $\text{Al}_{72}\text{Ni}_{12}\text{Co}_{16}$ quasicrystalline particles and the Al melt are a complex process and the detailed interfacial reaction mechanism will be reported in another article.

Effect of hot-extrusion on the microstructure

The microstructure and phase composition of the as-cast composite after annealed at 400 °C for 2 h has been examined by SEM, EDS, and XRD, which showed the similar feature to that of the as-cast composite. This can be attributed to the fact that the annealing temperature (400 °C) is reasonably lower than the solidus temperature (637.9 °C [21]) of Al–Ni–Co alloy.

To evaluate the porosity rate of both the as-cast composite and the composite after extrusion, the practical densities of these materials were measured, as summarized in Table 1. The theoretical density of the composite is also given in the table, which was calculated by the ROM using the density of Al (2.70 g/cm³) and the measured density of the $\text{Al}_{72}\text{Ni}_{12}\text{Co}_{16}$ alloy (3.84 g/cm³). It is evident from the table that the porosity of the Al matrix is increased by adding the reinforcement particles. The hot-extrusion results in a remarkable increase of the composite density, which is very close to the theoretical value (Table 1). In other words, the porosity of the composite is reduced by the hot-extrusion.

Due to the effect of the dendritic solidification of the matrix, the particle distribution in the as-cast composite is inevitably non-uniform. After the hot-extrusion, the distribution of the Al–Ni–Co particles is obviously modified and the particle size is slightly decreased (Fig. 4) as compared with that in the as-cast composite (Fig. 2a). In

Table 1 Results of density measurements

Sample	Practical density (± 0.01) (g/cm ³)	Theoretical density (g/cm ³)	Porosity (%)
As-cast Al	2.67	2.70	1.1
As-cast composite	2.77	2.82	1.8
Extruded composite	2.81		0.3

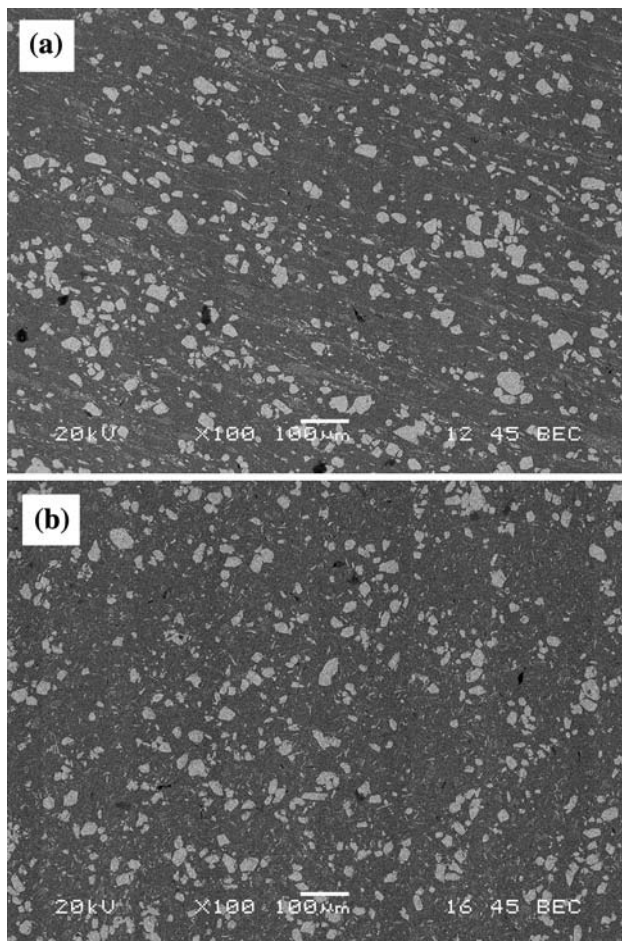


Fig. 4 BSE images of the extruded composite on sections along (a) and perpendicular to (b) the extrusion direction

addition, the eutectic structure in the Al matrix was broken and aligned along the extrusion direction (Fig. 4a). Similar results on the study of the effects of secondary extrusion process on the microstructures and porosities of ceramic particle reinforced metal matrix composites (PRMMCs) have been widely documented [13–15, 22–26].

Tensile properties and fracture examination

The tensile properties of both the as-cast Al matrix and the composites in as-cast state and after extrusion are shown in Fig. 5. Each value is an average of four measurements. The ultimate tensile strength (UTS), yield strength (YS), and elastic modulus (EM) of the as-cast composite are increased over the corresponding Al matrix properties by about 36%, 40%, and 10%, respectively, but the elongation to fracture (EF) is decreased. After the hot-extrusion, the UTS and EF of the composite are remarkably increased compared to the as-cast composite, while the increase of the YS is negligible and the EM is even slightly decreased.

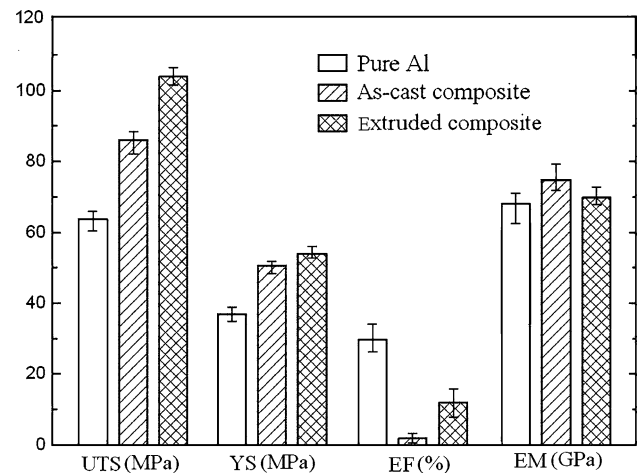


Fig. 5 Tensile properties of the tested Al matrix and the composites in different states

Figure 6a–d shows the fractographs and longitudinal-sections of the failed tensile samples from the as-cast and extruded composites. Micro-dimples in the Al matrix and ductile tearing ridges around the cracked particles can be seen from Fig. 6a, b. In addition, some particle cracking can be seen in the fracture surface of the extruded sample (as shown in Fig. 6b marked by rectangles). From the longitudinal-section images near the fracture surface of the as-cast and extruded samples (Fig. 6c, d), it is suggested that for the as-cast sample, fracture occurred through particle cracking and grain boundary separation, while as the case of the extruded sample, fracture occurred by particle cracking and matrix tearing. Decohesion at particle–matrix interface can not be found both in the as-cast and extruded samples, which confirms the good interfacial bonding between the Al matrix and the $\text{Al}_9(\text{Co}, \text{Ni})_2$ particles.

It can be concluded from the microstructure and fracture examination that the improvements of the UTS, YS, and EM of the as-cast composite are related to the fine particle size, good particle–matrix interfacial bonding and uniform distribution of the reinforcement particles in the matrix. In addition to the strengthening effect of the $\text{Al}_9(\text{Co}, \text{Ni})_2$ particles, the matrix strengthening due to solid solution of element Ni and Co and the existence of the $\text{Al}_3(\text{Ni}, \text{Co})$ phase may also have played an efficient role on the increase of the strength. The decrease of ductility with the addition of reinforcement particles is a prevalent phenomenon in PRMMCs [1, 22], which result from the elastic restraint imposed on the matrix by the un-deformable reinforcement particles and the cracking of the particles. Also, the microstructure defects such as particle clustering, shrinkage cavity, and porosity can degrade the ductility. In the present study, another factors contributing to the brittleness of the as-cast composite is the presence of eutectic phase

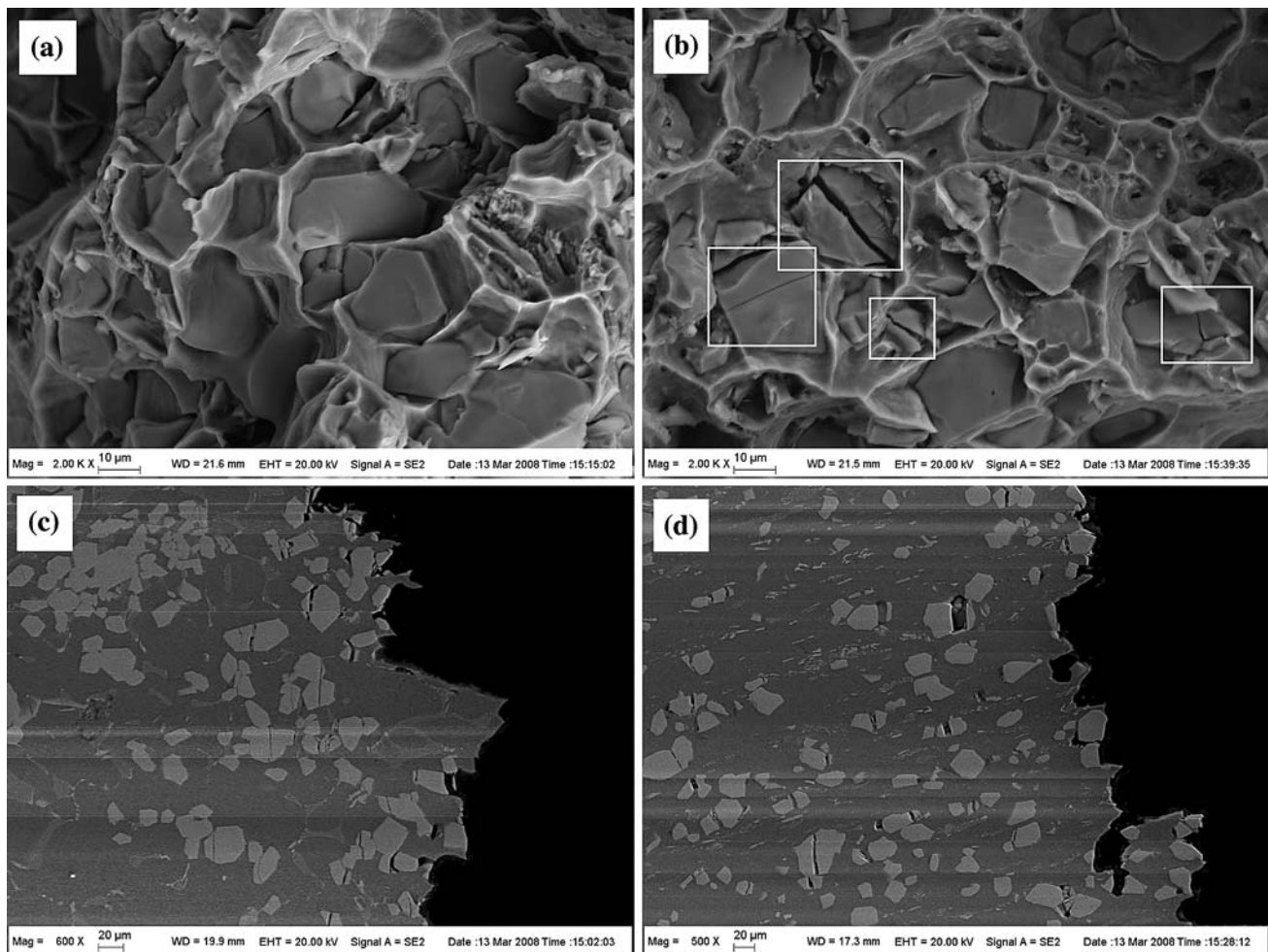


Fig. 6 SEM images of the fracture surfaces of the as-cast (a) and extruded (b) composites, and BSE images longitudinal-sections near the fracture surfaces of the as-cast (c) and extruded (d) composites

distributing along the matrix grain boundaries, as confirmed by the fracture examination (Fig. 6c).

It was widely recognized that hot-extrusion can increase the strength and ductility of PRMMCs [14, 22, 25]. The improvement in these properties was explained by the reduction in the porosity and the changes in the microstructure caused by extrusion [14, 22]. The observed increasing of the UTS and EF after the hot-extrusion in the present study can also be attributed to the above reasons. The microstructure changes appear mainly to be the homogenization of the reinforcement particle and eutectic phase distribution. In addition, some refinement of the matrix structure is expected to have occurred.

Besides the beneficial effects as mentioned above, the hot-extrusion is also found to bring about the formation of microporosity and particle breakage. Figure 7a, b show examples of the microporosity and multiple particle fractures, respectively, in the extruded composite. Particle cracking present in the fracture surface of the extruded

composite as shown in Fig. 6b can also confirm the statement. Multiple fractures of reinforcement particles arose from extrusion have also been reported by Tham et al. [23] and the formation mechanism was extensively interpreted. Davies et al. [26] pointed out that particle fracture is a potential defect of extruded composites if associated with void formation, which will especially degrade the elastic property of the composite. In the present study, those microstructure defects are, consequently, presumed to have decreased the EM of the extruded composite due to the fact that those defects cannot transfer shear and tensile stresses [27]. Also, the defects formed during the extrusion can decrease the YS of the composite. On the other hand, the modification of the reinforcement particle distribution and the reduction of the porosity are expected to improve the EM and YS [22, 28, 29]. The transfer of these two properties is a result of the combined effect of these inverse factors and dependent on which of these effects is dominant, the EM and YS are decreased or increased.

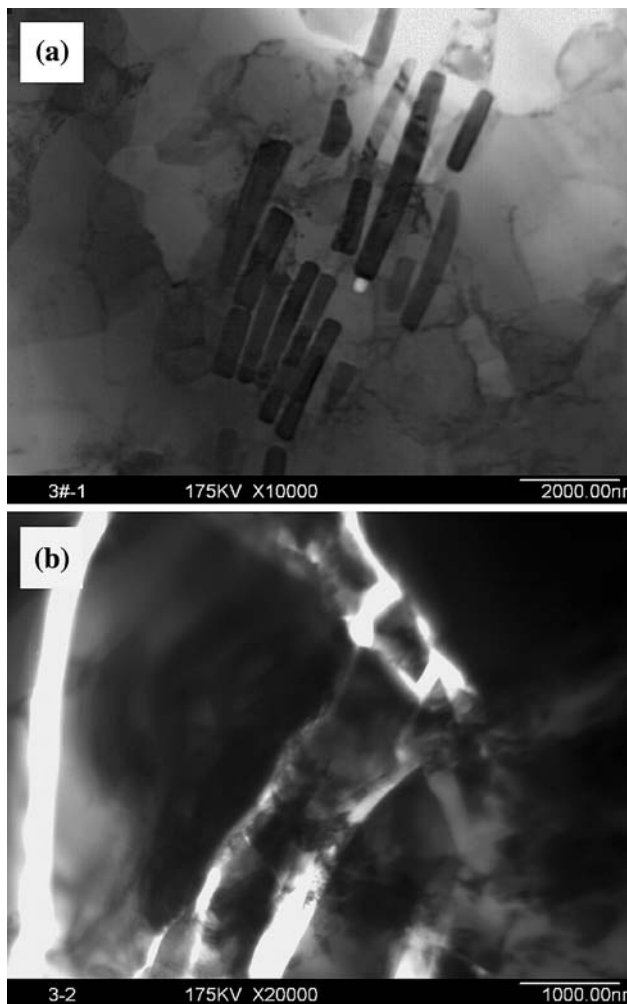


Fig. 7 TEM images showing microporosity formed near the fractured eutectic phases (a) and a fractured $\text{Al}_9(\text{Co}, \text{Ni})_2$ particle (b) in the extruded composite

General discussion

The strength and ductility of PRMMCs is frequently observed to be lower in the composites containing coarse reinforcement particles compared with the composites reinforced by fine particles if particle clustering can be avoided [9, 30]. However, the processing of the composites containing fine particles is relatively more difficult due to the reasons as described by Tham et al. [23]. In this study, by adding relatively coarse particles (100–150 μm), via interactions between the coarse particles and molten metal and the fragmentation of the reaction product, a fine particle (smaller than 50 μm) distributed AMC was obtained. As presented in the preceding sections, the resultant as-cast composite has a uniform particle distribution and a strong particle–matrix interfacial bonding, giving rise to an increased strength. Therefore, in terms of practical implications, our experimental practice suggests that the

interaction of a non-equilibrium system can be used to produce fine particle reinforced composites. Obviously, this method can overcome some of the difficulties of the processing of fine particle reinforced composites to a certain extent.

Conclusions

In the present study, $\text{Al}_{72}\text{Ni}_{12}\text{Co}_{16}$ single-QC was used to produce Al–Ni–Co IMC particle reinforced Al matrix composite by the usual stir-casting method. Hot-extrusion was performed to investigate the effect of the secondary process on the microstructure and the mechanical properties of the composite. From the analysis results, the following conclusions can be drawn.

1. The $\text{Al}_{72}\text{Ni}_{12}\text{Co}_{16}$ quasicrystalline particles have transformed to the crystalline phase $\text{Al}_9(\text{Co}, \text{Ni})_2$ and particle fragmentation has happened during the producing process, giving rise to a fine $\text{Al}_9(\text{Co}, \text{Ni})_2$ IMC particle reinforced AMC. The particle distribution is relatively uniform and the particle–matrix interfacial bonding in the as-cast composite is good.
2. The UTS, YS, and EM of the as-cast composite are increased over the corresponding Al matrix properties by about 36%, 40%, and 10%, respectively, while the EF is decreased. The strength and EM increases are considered to be attributed to the presence of fine reinforcement particles, uniform particle distribution, and good particle–matrix interfacial bonding along with the effect of solid solution strengthening of the matrix.
3. The hot-extrusion can further increase the UTS, especially the EF can be obviously increased due to the reduction of the porosity and the improved distribution of the reinforcement particles and eutectic structure. However, the YS and EM keep constant or even can be decreased, which should be related to the formation of microporosity and multiple particle fractures bring about by the extrusion.

Acknowledgements This work was supported by the National Natural Science Foundation of China (Grant No. 50571081) and the Aviation Foundation of China (Grant No. 04G53024).

References

1. Lloyd DJ (1994) *Int Mater Rev* 39:1
2. Tsai AP, Suenaga H, Ohmori M, Yokoyama Y, Inoue A, Masumoto T (1992) *Jpn J Appl Phys* 31:2530
3. Tsai AP, Aoki K, Inoue A, Masumoto T (1993) *J Mater Res* 8:5
4. Lee SM, Jung JH, Fleury E, Kim WT, Kim DH (2000) *Mater Sci Eng* 294–296:99

5. Tang F, Anderson IE, Gnaupel-Herold T, Prask H (2004) *Mater Sci Eng A* 383:362
6. Kaloshkin SD, Tcherdyntsev VV, Laptev AI (2004) *J Mater Sci* 39:5399. doi:[10.1023/B:JMSE.0000039253.28721.3f](https://doi.org/10.1023/B:JMSE.0000039253.28721.3f)
7. Tsai AP, Inoue A, Masumoto T (1989) *Mater Trans JIM* 30:463
8. Gödecke T, Scheffer M, Lück R, Ritsch S, Beeli C (1998) *Z Metallkd* 89:687
9. Poddar P, Srivastava VC, De PK, Sahoo KL (2007) *Mater Sci Eng A* 460–461:357
10. Bindumadhavan PN, Chia TK, Chandrasekaran M (2001) *Mater Sci Eng A* 315:217
11. Cöcen Ü, Önel K (1996) *Mater Sci Eng A* 221:187
12. Samuel AM, Gotmare A, Samuel FH (1995) *Compos Sci Technol* 53:301
13. Tekmen C, Ozdemir I, Cocen U, Onel K (2003) *Mater Sci Eng A* 360:365
14. Seo YH, Kang CG (1999) *Compos Sci Technol* 59:643
15. Rahmani Fard R, Akhlaghi F (2007) *J Mater Process Technol* 187–188:433
16. Onat A, Akbulut H, Yilmaz F (2007) *J Alloy Compd* 436:375
17. Shorowordi KM, Laoui T, Haseeb ASMA, Celis JP, Froyen L (2003) *J Mater Process Technol* 142:738
18. Banerji A, Surappa MK, Rohatgi PK (1983) *Metall Trans B* 14:273
19. Banerji A, Rohatgi PK (1982) *J Mater Sci* 17:335. doi:[10.1007/BF00591467](https://doi.org/10.1007/BF00591467)
20. Rohatgi PK, Pai BC, Panda SC (1979) *J Mater Sci* 14:2277. doi:[10.1007/BF00737014](https://doi.org/10.1007/BF00737014)
21. Raynor GV, Pfeil PCL (1947) *J Inst Metals* 73:609
22. Cöcen Ü, Önel K (2002) *Compos Sci Technol* 62:275
23. Tham LM, Gupta M, Cheng L (2002) *Mater Sci Eng A* 326:355
24. Davies CHJ, Chen W-S, Lloyd DJ, Hawbolt EB, Samarasekera IV, Brimacombe JK (1996) *Metall Mater Trans A* 274:113
25. Zhong WM, L'Espérance G, Suéry M (1996) *Mater Sci Eng A* 214:93
26. Davies CHJ, Chen W-S, Hawbolt EB, Samarasekera IV, Brimacombe JK (1995) *Scr Metall Mater* 32:309
27. Lloyd DJ (1991) *Acta Metall Mater* 39:59
28. Yi HZ, Ma NH, Zhang YJ, Li XF, Wang HW (2006) *Scr Mater* 54:1093
29. Tham LM, Su L, Cheng L, Gupta M (1999) *Mater Res Bull* 34:71
30. Tan MJ, Koh LH, Khor KA, Boey FYC (1993) *J Mater Process Technol* 37:391